Kinematic power corrections to deeply virtual Compton scattering to twist-six accuracy

V. M. Braun,[1] Yao Ji,[2,3] and A. N. Manashov[4,1]

[1]*Institut für Theoretische Physik, Universität Regensburg, D-93040 Regensburg, Germany*
[2]*School of Science and Engineering, The Chinese University of Hong Kong, Shenzhen 518172, China*
[3]*Physics Department T31, Technische Universität München, D-85748 Garsching, Germany*
[4]*II. Institut für Theoretische Physik, Universität Hamburg, D-22761 Hamburg, Germany*

(Received 21 January 2025; accepted 31 March 2025; published 14 April 2025)

We calculate $(\sqrt{-t}/Q)^k$ and $(m/Q)^k$ power corrections with $k \leq 4$, where m is the target mass and t is the momentum transfer, to several key observables in deeply virtual Compton scattering (DVCS). We find that the power expansion is well convergent up to $|t|/Q^2 \lesssim 1/4$ for most of the observables, but is naturally organized in terms of $1/(Q^2+t)$ rather than the nominal hard scale $1/Q^2$. We also argue that target mass corrections remain under control and do not endanger quantum chromodynamics (QCD) factorization for coherent DVCS on nuclei. These results remove an important source of uncertainties due to the frame dependence and violation of electromagnetic Ward identities in the QCD predictions for the DVCS amplitudes in the leading-twist approximation.

DOI: 10.1103/PhysRevD.111.076011

I. INTRODUCTION

Studies of the deeply virtual Compton scattering (DVCS) play an important role in the quest for the three-dimensional "tomographic" imaging of the proton and light nuclei. This reaction gives access to the generalized parton distributions (GPDs) [1–3] that encode the information on the transverse position of quarks and gluons in the proton in dependence on their longitudinal momentum. This is an active research topic and a major science goal for the planned Electron-Ion Collider (EIC) [4,5]. The QCD description of the DVCS is based on collinear factorization. At leading power, the complete next-to-leading-order (NLO) results are available since long ago [6–9]. A lot of effort is put into extending this description to NNLO [10–20].

Beyond the leading twist, power-suppressed contributions $\sim(\sqrt{-t}/Q)^k$ and $\sim(m/Q)^k$, where t is the invariant momentum transfer and m is the target mass, play a special role. They can be large and have to be taken into account. Indeed, the transverse spatial position of partons in the target is Fourier conjugate to the momentum transfer in the scattering process. Hence the resolving power of DVCS is directly limited by the range of the invariant moment transfer t which can be used in the analysis. Theoretical control over power corrections $(\sqrt{-t}/Q)^k$ is therefore crucial for three-dimensional imaging. One more pressing issue is to clarify whether target mass corrections $\sim(m/Q)^k$ do not endanger QCD factorization for coherent DVCS on nuclei [21,22].

We refer to the $\sim(\sqrt{-t}/Q)^k$ and $\sim(m/Q)^k$ contributions to Compton amplitudes as "kinematic power corrections" because they do not involve new nonperturbative inputs in addition to the leading twist GPDs. On an intuitive level, their origin and interpretation can be explained as follows [23]. The four-momenta of the initial and final photons and nucleons in a DVCS process do not lie in one plane. Hence the distinction of longitudinal and transverse directions is convention-dependent and, as a consequence, the leading-twist approximation is intrinsically ambiguous. In the Bjorken limit this is a $1/Q$ effect. On a more technical level, the freedom to redefine large "plus" parton momenta by adding small transverse components has two consequences. First, the dependence of the skewness parameter ξ on the Bjorken variable x_B acquires t-dependent power suppressed contributions. Second, such a redefinition generally leads to excitations of the subleading photon helicity-flip amplitudes [23,24]. This convention-dependence proves to be rather large, see [25] for a detailed study. It should be viewed as a theoretical uncertainty that can and should be removed by explicit calculation of the kinematic power corrections and adding them to the leading-twist expressions in the data analysis.

This problem was addressed in [26–29], where a technique was developed that allows one to calculate kinematic corrections to the twist-four accuracy, i.e., up

to terms $\sim t/Q^2$ and $\sim m^2/Q^2$. The results in the final form were presented in [24]. A typical size of kinematic corrections for $|t|/Q^2 \lesssim 1/4$ was found to be of the order of 10% for asymmetries, but they could be as large as 100% for the DVCS cross section in certain kinematics. These corrections can significantly impact the extraction of GPDs from data and have to be taken into account [30–32].

The approach of [26–29] requires explicit construction of the higher-twist operator basis and becomes unwieldy beyond twist four. In Ref. [33] we suggested a different technique to calculate kinematic corrections to generic two-photon processes, based on the conformal field theory (CFT) methods. This technique is more general and is applicable to all twists. Using this new approach we have calculated in Ref. [34] the kinematic power corrections to twist-six accuracy for the simplest case of DVCS on a scalar target. In this work we derive the corresponding expressions for the spin-1/2 targets (nucleon). We achieve the following accuracy, schematically:

$$\begin{aligned}\mathcal{A}^{(\pm,\pm)} &\sim 1+\frac{1}{Q^2}+\frac{1}{Q^4},\\ \mathcal{A}^{(\pm,0)} &\sim \frac{1}{Q}+\frac{1}{Q^3},\\ \mathcal{A}^{(\pm,\mp)} &\sim \frac{1}{Q^2}+\frac{1}{Q^4},\end{aligned} \tag{1}$$

where $\mathcal{A}^{(\pm,\pm)}$, $\mathcal{A}^{(\pm,0)}$, and $\mathcal{A}^{(\pm,\mp)}$ are the helicity-conserving, helicity-flip and double-helicity-flip amplitudes, respectively. Precise definitions are given in the text. Taking into account these corrections removes the frame dependence of the leading-twist approximation and restores the electromagnetic gauge invariance of the Compton amplitude up to $1/Q^5$ effects.

Besides providing general expressions, we study the numerical impact of kinematic corrections on several key experimental DVCS observables. We find that the twist-five and twist-six contributions can be decreased by changing the expansion parameter in the twist-three and twist-four corrections from the photon virtuality Q^2 to Q^2+t. In addition, we confirm the observation made in [24] that target mass corrections always involve powers of the skewness parameter $\sim(\xi m/Q)^k$ and do not endanger QCD factorization for coherent DVCS on nuclei.

II. BMP HELICITY AMPLITUDES

A. Definitions and conventions

In this work we consider DVCS on the nucleon target

$$\gamma^*(q)+N(p,s)\longrightarrow\gamma(q')+N(p',s'). \tag{2}$$

The DVCS amplitude $\mathcal{A}_{\mu\nu}$ is defined as

$$\begin{aligned}&\mathcal{A}_{\mu\nu}(q,q',p)\\ &=i\int d^4x e^{-i(z_1q-z_2q')\cdot x}\langle p',s'|T\{j_\mu(z_1x)j_\nu(z_2x)\}|p,s\rangle,\end{aligned} \tag{3}$$

where $j_\mu(z_1x)$ and $j_\nu(z_2x)$ are the electromagnetic currents, z_1, z_2 are real numbers such that $z_1-z_2=1$. Note that $\mathcal{A}_{\mu\nu}$ does not depend on z_1+z_2. This property is referred to as translation invariance in Refs. [28,29]. It is violated at the leading twist and is restored by adding kinematic power corrections to the required accuracy.

We follow the BMP convention [28,29] and use the photon momenta, q and q', to define a longitudinal plane spanned by the two lightlike vectors

$$n=q',\qquad \tilde{n}=-q+(1-\tau)q', \tag{4}$$

where $\tau=t/(Q^2+t)$ with $Q^2=-q^2$. For this choice the momentum transfer to the target

$$\Delta=p'-p=q-q',\qquad t=\Delta^2$$

is purely longitudinal and both—initial and final state—proton momenta have a nonzero transverse component

$$P_\mu=\frac{1}{2}(p+p')=\frac{1}{2\xi}(\bar{n}_\mu-\tau n_\mu)+P_{\perp,\mu}. \tag{5}$$

The skewness parameter ξ is defined as

$$\xi\equiv\xi^{\rm BMP}=-\frac{\Delta\cdot q'}{2P\cdot q'}=\frac{x_B(1+t/Q^2)}{2-x_B(1-t/Q^2)} \tag{6}$$

and $|P_\perp|^2$ can be written in terms of kinematic invariants as

$$|P_\perp|^2=\frac{1-\xi^2}{4\xi^2}(t_{\rm min}-t),\qquad t_{\rm min}=-\frac{4m^2\xi^2}{1-\xi^2}. \tag{7}$$

The BMP choice is advantageous mainly because it leads to simple expressions for the photon polarization vectors that can be chosen as follows:

$$\begin{aligned}\varepsilon^0_\mu&=-(q_\mu-q'_\mu q^2/(q\cdot q'))/\sqrt{-q^2},\\ \varepsilon^\pm_\mu&=(P^\perp_\mu\pm i\bar{P}^\perp_\mu)/(\sqrt{2}|P_\perp|),\end{aligned} \tag{8}$$

where $P^\perp_\mu=g^\perp_{\mu\nu}P^\nu$, $\bar{P}^\perp_\mu=\varepsilon^\perp_{\mu\nu}P^\nu$ and

$$\begin{aligned}g^\perp_{\mu\nu}&=g_{\mu\nu}-(q_\mu q'_\nu+q'_\mu q_\nu)/(q\cdot q')+q'_\mu q'_\nu q^2/(q\cdot q')^2,\\ \varepsilon^\perp_{\mu\nu}&=\varepsilon_{\mu\nu\alpha\beta}q^\alpha q'^\beta/(q\cdot q'),\qquad \varepsilon^{\rm BMP}_{0123}=1.\end{aligned} \tag{9}$$

Normalization is such that $\varepsilon^+_\mu\varepsilon^{-\mu}=-1$, $\varepsilon^0_\mu\varepsilon^{0\mu}=+1$. The pair $\varepsilon^\pm_\mu$ form a basis in the transverse plane whereas ε^0_μ is a unit vector in longitudinal plane orthogonal to the photon momentum q'.

The DVCS amplitude $\mathcal{A}_{\mu\nu}$ can be decomposed in terms of scalar (helicity) amplitudes using this basis

$$\mathcal{A}_{\mu\nu} = \varepsilon^+_\mu \varepsilon^-_\nu \mathcal{A}^{++} + \varepsilon^-_\mu \varepsilon^+_\nu \mathcal{A}^{--} + \varepsilon^0_\mu \varepsilon^-_\nu \mathcal{A}^{0+} + \varepsilon^0_\mu \varepsilon^+_\nu \mathcal{A}^{0-} + \varepsilon^+_\mu \varepsilon^+_\nu \mathcal{A}^{+-} + \varepsilon^-_\mu \varepsilon^-_\nu \mathcal{A}^{-+}. \quad (10)$$

We neglected a term proportional to q'_ν since it does not contribute to any observable. Each helicity amplitude involves the sum over quark flavors, $\mathcal{A} = \sum e_q^2 \mathcal{A}_q$, and is written in terms of the leading-twist GPDs $H^q, E^q, \tilde{H}^q, \tilde{E}^q$. For the GPD definitions (see below), we follow Ref. [35].

B. Light-ray OPE

The amplitude $\mathcal{A}_{\mu\nu}$ can be written in terms of matrix elements of $C = +1$ twist-2 quark-antiquark light-ray operators

$$\mathcal{O}_V(z_1 y, z_2 y) = \frac{1}{2}\langle p'|[\bar{q}(z_1 y)\not{y} q(z_2 y)]_{\ell t} - (z_1 \leftrightarrow z_2)|p\rangle,$$
$$\mathcal{O}_A(z_1 y, z_2 y) = \frac{1}{2}\langle p'|[\bar{q}(z_1 y)\not{y}\gamma_5 q(z_2 y)]_{\ell t} + (z_1 \leftrightarrow z_2)|p\rangle, \quad (11)$$

where on the l.h.s. only the dependence on the quark positions is shown in order not to overload notation. In these expressions the Wilson line connecting the quarks is implied, and the notation $[\ldots]_{\ell t}$ stands for the leading twist projection as defined in Ref. [36]. The matrix elements (11) can be written in terms of the GPDs as follows:

$$\mathcal{O}_V(z_1 y, z_2 y) = \int_{-1}^1 dx [y^\rho e^{-i(Py)[z_1(\xi - x) + z_2(x+\xi)]}]_{\ell.t.} \times \{h_\rho H(x,\xi,t) + e_\rho E(x,\xi,t)\},$$
$$\mathcal{O}_A(z_1 y, z_2 y) = \int_{-1}^1 dx [y^\rho e^{-i(Py)[z_1(\xi - x) + z_2(x+\xi)]}]_{\ell.t.} \times \{\tilde{h}_\rho \tilde{H}(x,\xi,t) + \tilde{e}_\rho \tilde{E}(x,\xi,t)\}. \quad (12)$$

In these expressions we use shorthand notations [37] for the Dirac spinor bilinears

$$h_\rho = \bar{u}(p')\gamma_\rho u(p), \qquad \tilde{h}_\rho = \bar{u}(p')\gamma_\rho\gamma_5 u(p),$$
$$e_\rho = \bar{u}(p')\frac{i\sigma^{\rho\alpha}\Delta_\alpha}{2m}u(p), \qquad \tilde{e}_\rho = \frac{\Delta_\rho}{2m}\bar{u}(p')\gamma_5 u(p). \quad (13)$$

The leading twist projection of the exponential function is given by [38]

$$[e^{-i\ell y}]_{lt} = e^{-i\ell xy} + \frac{1}{4}y^2\ell^2\int_0^1 dt t e^{-it\ell y} + \frac{1}{32}y^4\ell^4\int_0^1 dt\bar{t}t^2 e^{-it\ell y} + \mathcal{O}(y^6),$$
$$[y^\rho e^{-i\ell y}]_{lt} = i\frac{\partial}{\partial \ell_\rho}[e^{-i\ell y}]_{lt}, \qquad \bar{t} = 1 - t. \quad (14)$$

The calculation of the DVCS amplitude in terms of the matrix elements of light-ray operators uses conformal symmetry techniques and is explained in Refs. [33,34]. Separating the contributions of the vector and axial-vector operators, $\mathcal{A}^{\mu\nu} = \mathcal{A}^{\mu\nu}_V + \mathcal{A}^{\mu\nu}_A$, we obtain

$$\mathcal{A}^{\mu\nu}_V = \int \frac{d^4x}{\pi^2}\frac{e^{-iqx}}{(-x^2+i0)}\int_0^1 d\alpha\int_0^{\bar{\alpha}} d\beta\Big\{\frac{1}{(-x^2+i0)}(g^{\mu\nu}\delta(\alpha)\delta(\beta) - x^\mu\partial^\nu\delta(\beta) - x^\nu\nabla^\mu\delta(\alpha))\mathcal{O}_V - \frac{i}{2}(\Delta^\nu\partial^\mu - \Delta^\mu\partial^\nu)\mathcal{O}_V$$
$$+\frac{1}{4}g^{\mu\nu}(\mathcal{O}_V^{(1)} - \delta(\alpha)\mathcal{O}_V^{(2)}) + \frac{1}{4}(x^\nu\partial^\mu + x^\mu\nabla^\nu)\left(\ln\bar{\tau}\mathcal{O}_V^{(1)} + \frac{\beta}{\bar{\beta}}\mathcal{O}_V^{(2)}\right) + \frac{1}{2}(x^\nu\partial^\mu - x^\mu\nabla^\nu)\frac{\tau}{\bar{\tau}}\left(-\mathcal{O}_V^{(1)} + \frac{\bar{\alpha}}{\alpha}\mathcal{O}_V^{(2)}\right)$$
$$-\frac{1}{4}x^\nu\nabla^\mu\frac{\beta}{\bar{\beta}}\left[4\left(\frac{1}{2}+\frac{\tau}{\bar{\tau}}\right)\mathcal{O}_V^{(1)} - \left(\delta(\alpha)+\frac{\beta}{\bar{\beta}}\right)\mathcal{O}_V^{(2)}\right] - \frac{x^\mu x^\nu}{(-x^2+i0)}\left[(\ln\bar{\tau}+\ln\bar{\alpha}+1)\mathcal{O}_V^{(1)} + \frac{\beta}{\bar{\beta}}\mathcal{O}_V^{(2)}\right]$$
$$+\frac{1}{2}x^\mu\partial^\nu\left[\ln\bar{\alpha}\mathcal{O}_V^{(1)} + \left(\frac{1}{2}-\frac{2\tau}{\bar{\tau}}\right)\mathcal{O}_V^{(2)}\right] + \frac{x^\mu x^\nu}{4}\left[\left(i(\Delta\partial)+\frac{\Delta^2}{2}\right)\frac{\beta}{\bar{\beta}}\left(\frac{2}{\bar{\tau}}-1\right) - 2\left(i(\Delta\partial)+\frac{\Delta^2}{4}\right)\left(\ln\bar{\tau}+\frac{2\tau}{\bar{\tau}}\right)\right]\mathcal{O}_V^{(1)}\Big\}, \quad (15)$$

and

$$\mathcal{A}^{\mu\nu}_A = \frac{1}{2}\int\frac{d^4x}{\pi^2}\frac{e^{-iqx}}{(-x^2+i0)}\int_0^1 d\alpha\int_0^{\bar{\alpha}} d\beta\Big\{i\varepsilon_{\mu\nu\beta\gamma}x^\beta\Big[\frac{1}{(-x^2+i0)}(-\nabla^\gamma\delta(\alpha) - \partial^\gamma\delta(\beta))\mathcal{O}_A$$
$$+\frac{1}{4}\nabla^\gamma\left(\left(\ln\bar{\tau} - \frac{2\beta}{\bar{\beta}}\right)\mathcal{O}_A^{(1)} + \frac{\beta}{\bar{\beta}}\left(1 + \delta(\alpha) - \frac{\beta}{\bar{\beta}}\right)\mathcal{O}_A^{(2)}\right) + \frac{1}{4}\partial^\gamma\left((\ln\bar{\tau} + 2\ln\bar{\alpha})\mathcal{O}_A^{(1)} + \frac{1}{\bar{\beta}}\mathcal{O}_A^{(2)}\right)\Big]$$
$$+(x_\nu\varepsilon_{\mu\alpha\beta\gamma} + x_\mu\varepsilon_{\nu\alpha\beta\gamma})x^\alpha\Delta^\gamma\partial^\beta\left[\frac{1}{(-x^2+i0)}\mathcal{O}_A - \frac{1}{4}\left(\ln\bar{\tau}\mathcal{O}_A^{(1)} + \frac{\beta}{\bar{\beta}}\mathcal{O}_A^{(2)}\right)\right]\Big\}, \quad (16)$$

where

$$\mathcal{O}_X^{(1)}(z_1x, z_2x) = i(\Delta\partial)\mathcal{O}_X(z_1x, z_2x),$$
$$\mathcal{O}_X^{(2)}(z_1x, z_2x) = \left(i(\Delta\partial) + \frac{\Delta^2}{2}\right)\mathcal{O}_X(z_1x, z_2x), \quad (17)$$

with $X = A$, V and

$$\tau = \frac{\alpha\beta}{\bar\alpha\,\bar\beta}, \qquad \partial^\gamma = \frac{\partial}{\partial x_\gamma}, \qquad \nabla^\gamma = \partial^\gamma - i\Delta^\gamma. \quad (18)$$

For brevity, we do not show the arguments of the operator matrix elements, which are the same for all cases, $\mathcal{O}_X$ stands for $\mathcal{O}_X(\bar\alpha x, \beta x)$. The expression in (15) is equivalent to that given in Ref. [34]; the contribution of axial-vector operators in (16) is a new result.

C. Results

In this section we denote vector and axial-vector Dirac bispinors as

$$v^\mu = \bar u(p')\gamma^\mu u(p),$$
$$a^\mu = \bar u(p')\gamma^\mu\gamma_5 u(p), \quad (19)$$

and use shorthand notations [39] for the scalar products with the BMP polarization vectors defined in (8)

$$v_\perp^\pm = (v\cdot\varepsilon^\pm), \qquad a_\perp^\pm = (a\cdot\varepsilon^\pm),$$
$$P_\perp^\pm = (P\cdot\varepsilon^\pm) = -|P_\perp|/\sqrt{2}. \quad (20)$$

At the intermediate stages of the calculation the "double distribution" (DD) [3] parametrization of the nucleon matrix elements of light-ray vector- and axial-vector operators proves to be the most convenient. The results in the DD representation are collected in the Appendix.

In the following expressions we use rescaled variables

$$\hat t = \frac{t}{(qq')}, \qquad \hat m^2 = \frac{m^2}{(qq')}, \qquad |\hat P_\perp|^2 = \frac{|P_\perp|^2}{(qq')}, \quad (21)$$

where $(qq') = -1/2(Q^2 + t)$. We use the notation

$$M(x,\xi,t) = H(x,\xi,t) + E(x,\xi,t), \quad (22)$$

and

$$D_\xi = (-2\xi^2\partial_\xi). \quad (23)$$

It is convenient to use different normalization for the convolution integrals of the coefficient functions with different GPDs

$$(M\otimes T) = \int dx M(x,\xi,t)T\left(\frac{x+\xi}{2\xi}\right),$$
$$(\tilde H\otimes T) = \int dx \tilde H(x,\xi,t)T\left(\frac{x+\xi}{2\xi}\right),$$
$$(E\odot T) = \frac{1}{2\xi}\int dx E(x,\xi,t)T\left(\frac{x+\xi}{2\xi}\right),$$
$$(\tilde E\circledast T) = \frac{1}{2}\int dx \tilde E(x,\xi,t)T\left(\frac{x+\xi}{2\xi}\right). \quad (24)$$

The coefficient functions appearing in the equations below are defined as

$$T_0(z) = \frac{1}{\bar z}, \qquad T_1(z) = \ln\bar z,$$
$$T_{00}(z) = \frac{\bar z}{z}\ln\bar z, \qquad T_{10}(z) = \frac{1}{z}\ln\bar z,$$
$$T_{11}(z) = \left(2 - \frac{1}{z}\right)\ln\bar z,$$
$$T_V(z) = \frac{1}{\bar z}(\mathrm{Li}_2(z) - \zeta_2) - \ln\bar z,$$
$$T_A(z) = -\frac{1}{\bar z}(\mathrm{Li}_2(z) - \zeta_2) + \frac{1}{z}\ln\bar z,$$
$$T_2(z) = \frac{1}{\bar z}(\mathrm{Li}_2(z) - \zeta_2) - \frac{1}{2z}\ln\bar z,$$
$$T_3(z) = \frac{2z+1}{\bar z}(\mathrm{Li}_2(z) - \zeta_2) - \frac{1}{2}\left(7 - \frac{1}{z}\right)\ln\bar z. \quad (25)$$

They are analytic functions of z with a cut from 1 to ∞, apart from T_0 which has a pole singularity. Functions of higher transcendentality appear at intermediate steps of the calculation but cancel in the final expressions. The convolution integrals (24) involve the CFs on the upper side of the cut: $T(z) \mapsto T(z + i\varepsilon)$ for $x > \xi > 0$.

1. *Helicity-conserving* $(\pm,\pm)$ *amplitude*

We obtain

$$\mathcal{A}_V^{\pm,\pm} = \frac{(vq')}{(qq')}V_0^{(1)} + \frac{(vP)}{m^2}V_0^{(2)},$$
$$\mathcal{A}_A^{\pm,\pm} = \pm\frac{(aq')}{(qq')}A_0^{(1)} \pm \frac{(a\Delta)}{2m^2}A_0^{(2)}, \quad (26)$$

where

$$
\begin{aligned}
V_0^{(1)} &= -\left(1+\frac{\hat{t}}{4}\right)(M\otimes T_0) - \frac{\hat{t}}{2}(M\otimes T_{10}) + \frac{1}{4}\hat{t}^2(M\otimes T_{11}) - \frac{1}{2}D_\xi^2|\hat{P}_\perp|^2(M\otimes(T_2+2\hat{t}T_V)) + \frac{1}{8}D_\xi^3|\hat{P}_\perp|^4 D_\xi(M\otimes T_3),\\
V_0^{(2)} &= -\left(1+\frac{\hat{t}}{4}\right)(E\odot T_0) - \frac{\hat{t}}{2}(E\odot T_{10}) + \frac{\hat{t}^2}{4}(E\odot T_{11}) - \frac{1}{2}D_\xi|\hat{P}_\perp|^2 D_\xi(E\odot(T_2+2\hat{t}T_V)) + \frac{1}{8}D_\xi^2|\hat{P}_\perp|^4 D_\xi^2(E\odot T_3)\\
&\quad - \hat{m}^2\left\{D_\xi(M\otimes(T_2+2\hat{t}T_V)) - \frac{1}{2}D_\xi^2|\hat{P}_\perp|^2(M\otimes T_3)\right\},\\
A_0^{(1)} &= \left(1+\frac{\hat{t}}{4}\right)(\tilde{H}\otimes T_0) + \frac{\hat{t}}{2}\left(1+\frac{\hat{t}}{2}\right)(\tilde{H}\otimes T_{10}) + \frac{1}{2}D_\xi^2|\hat{P}_\perp|^2(\tilde{H}\otimes(T_2-2\hat{t}T_A)) - \frac{3}{16}D_\xi^3|\hat{P}_\perp|^4 D_\xi(\tilde{H}\otimes(T_{00}-2T_A)),\\
A_0^{(2)} &= \left(1+\frac{\hat{t}}{4}\right)(\tilde{E}\circledast T_0) + \frac{\hat{t}}{2}(\tilde{E}\circledast T_{10}) + \frac{\hat{t}^2}{4}\left(\tilde{E}\circledast\left(T_{10}+\frac{3}{2}\right)\right) + \frac{1}{2}D_\xi|\hat{P}_\perp|^2 D_\xi(\tilde{E}\circledast(T_2-2\hat{t}T_A))\\
&\quad - \frac{3}{16}D_\xi^2|\hat{P}_\perp|^4 D_\xi^2(\tilde{E}\circledast(T_{00}-2T_A)) + \hat{m}^2 D_\xi\left\{\frac{1}{\xi}(\tilde{H}\otimes(T_2-2\hat{t}T_A)) - \frac{3}{4}D_\xi\frac{1}{\xi}|\hat{P}_\perp|^2 D_\xi(\tilde{H}\otimes(T_{00}-2T_A))\right\}. \qquad (27)
\end{aligned}
$$

We have verified that the invariant amplitudes $(V_0^{(1)}, V_0^{(2)})$ and $(A_0^{(1)}, A_0^{(2)})$ coincide with $(\mathbb{V}_2/2, \mathbb{V}_1)$ and $(\mathbb{A}_2/2, \mathbb{A}_1)$ as defined in Ref. [24] [Eq. (A15)], up to twist-six terms $\hat{t}^2, \hat{t}\hat{m}^2, \ldots$, respectively.

2. Helicity-flip $(\mathbf{0},\pm)$ amplitude

This is a subleading-power amplitude that starts at the twist-3 level. We obtain

$$
\begin{aligned}
\mathcal{A}_V^{0,\pm} &= \frac{Q}{(qq')}\left(v_\pm V_1^{(1)} + \frac{(vq')P_\pm}{(qq')}V_1^{(2)} + \frac{(vP)P_\pm}{m^2}V_1^{(3)}\right),\\
\mathcal{A}_A^{0,\pm} &= \pm\frac{Q}{(qq')}\left(a_\pm A_1^{(1)} + \frac{(aq')P_\pm}{(qq')}A_1^{(2)} + \frac{(a\Delta)P_\pm}{2m^2}A_1^{(3)}\right)
\end{aligned} \qquad (28)
$$

with

$$
\begin{aligned}
V_1^{(1)} &= -\left(1+\frac{\hat{t}}{2}\right)(M\otimes T_{10}) + \hat{t}(M\otimes T_1) - \frac{1}{2}D_\xi^2|\hat{P}_\perp|^2(M\otimes T_V),\\
V_1^{(2)} &= -D_\xi V_1^{(1)},\\
V_1^{(3)} &= \left(1+\frac{\hat{t}}{2}\right)D_\xi(E\odot T_{10}) - \hat{t}D_\xi(E\odot T_1) + \frac{1}{2}D_\xi^2|\hat{P}_\perp|^2 D_\xi(E\odot T_V) + \hat{m}^2 D_\xi^2(M\otimes T_V),\\
A_1^{(1)} &= \left(1+\frac{\hat{t}}{2}\right)(\tilde{H}\otimes T_{10}) - \frac{1}{2}D_\xi^2|\hat{P}_\perp|^2(\tilde{H}\otimes T_A),\\
A_1^{(2)} &= -D_\xi A_1^{(1)},\\
A_1^{(3)} &= -\left(1+\frac{\hat{t}}{2}\right)D_\xi(\tilde{E}\circledast T_{10}) + \frac{1}{2}D_\xi^2|\hat{P}_\perp|^2 D_\xi(\tilde{E}\circledast T_A) + \hat{m}^2 D_\xi^2\frac{1}{\xi}(\tilde{H}\otimes T_A).
\end{aligned} \qquad (29)
$$

To twist-three accuracy (leading terms), these expressions agree with Ref. [24] [Eq. (A16)].

3. Double-helicity-flip $(\mp,\pm)$ amplitude

$$
\begin{aligned}
\mathcal{A}_V^{\mp\pm} &= \frac{v_\pm P_\pm}{(qq')}V_2^{(1)} + \frac{(vq')}{(qq')}V_2^{(2)} + \frac{(vP)}{m^2}V_2^{(3)},\\
\mathcal{A}_A^{\mp\pm} &= \pm\frac{a_\pm P_\pm}{(qq')}A_2^{(1)} \pm \frac{(aq')}{(qq')}A_2^{(2)} \pm \frac{(a\Delta)}{2m^2}A_2^{(3)}.
\end{aligned} \qquad (30)
$$

We get

$$
\begin{aligned}
V_2^{(1)} &= 2\left(1+\frac{\hat{t}}{4}\right)D_\xi(M\otimes T_{11}) - \frac{1}{2}D_\xi^3|\hat{P}_\perp|^2(M\otimes T_V),\\
V_2^{(2)} &= -\frac{1}{4}|\hat{P}_\perp|^2 D_\xi V_2^{(1)},\\
V_2^{(3)} &= -\frac{1}{2}|\hat{P}_\perp|^2 D_\xi^2\left\{\left(1+\frac{\hat{t}}{4}\right)(E\odot T_{11}) - \frac{1}{4}D_\xi|\hat{P}_\perp|^2 D_\xi(E\odot T_V) - \frac{1}{2}\hat{m}^2 D_\xi(M\otimes T_V)\right\},\\
A_2^{(1)} &= 2\left(1+\frac{\hat{t}}{4}\right)D_\xi(\tilde{H}\otimes T_{10}) - \frac{1}{2}D_\xi^3|\hat{P}_\perp|^2(\tilde{H}\otimes T_A),\\
A_2^{(2)} &= -\frac{1}{4}|\hat{P}_\perp|^2 D_\xi A_2^{(1)},\\
A_2^{(3)} &= -\frac{1}{2}|\hat{P}_\perp|^2 D_\xi^2\left\{\left(1+\frac{\hat{t}}{4}\right)(\tilde{E}\circledast T_{10}) - \frac{1}{4}D_\xi|\hat{P}_\perp|^2 D_\xi(\tilde{E}\circledast T_A) - \frac{1}{2}\hat{m}^2 D_\xi\frac{1}{\xi}(\tilde{H}\otimes T_A)\right\}.
\end{aligned}
\tag{31}
$$

At leading order (twist four), these expressions agree with the corresponding results in [24] [Eq. (A17)], except for the sign of the $A_2^{(3)}$ contribution. In the DD representation [24] [Eq. (B11)] all results agree.

One of the motivations for our study was to clarify whether target mass corrections $\sim(m/Q)^k$ do not endanger QCD factorization for coherent DVCS on nuclei [21,22]. By inspection of the above equations, one can check that target mass dependent contributions always involve additional factors of the skewness parameter, so that the expansion goes in powers of $\xi^2 m^2/Q^2$ rather than m^2/Q^2. For nuclear targets, effectively, $m\to Am$ and $\xi\to\xi/A$, so that the target mass corrections remain essentially the same as for the nucleon and are small, apart from the large x_B region.

III. COMPTON FORM FACTORS AND THE FRAME DEPENDENCE

Compton form factors (CFFs) are defined [40] through the decomposition of the helicity amplitudes in terms of the set of bilinear spinors in Eq. (13)

$$
\mathcal{A}^{a,\pm}_{\rm BMP} = \mathcal{H}^{a,\pm}_{\rm BMP}h + \mathcal{E}^{a,\pm}_{\rm BMP}e \mp \tilde{\mathcal{H}}^{a,\pm}_{\rm BMP}\tilde{h} \mp \tilde{\mathcal{E}}^{a,\pm}_{\rm BMP}\tilde{e}, \tag{32}
$$

where $a=(+,0,-)$ and we have reintroduced the notation "BMP" to remind that the helicity amplitudes and hence also the CFFs are defined using BMP conventions, see Sec. II A. Making use of the Dirac equation for the nucleon states, one finds [24]

$$
\begin{aligned}
&\frac{(vP)}{2m^2} = h-e, \quad \frac{(vq')}{qq'} = -\frac{1}{\xi}h,\\
&\frac{(a\Delta)}{4m^2} = -\frac{1}{\xi}\left(1+\frac{t}{Q^2}\right)\tilde{e}, \quad \frac{(aq')}{(qq')} = -\frac{1}{\xi}\tilde{h} - \frac{1}{\xi}\frac{4m^2}{Q^2}\tilde{e},
\end{aligned}
\tag{33}
$$

and

$$
\begin{aligned}
\frac{v_\perp^\pm}{\sqrt{2}} &= -|P_\perp|h - \frac{m^2}{|P_\perp|}\left[e - \frac{t}{4m^2}h\right] \mp \frac{m^2}{\xi|P_\perp|}\left[\tilde{e} - \frac{t}{4m^2}\tilde{h}\right],\\
\frac{a_\perp^\pm}{\sqrt{2}} &= -\frac{m^2}{\xi^2|P_\perp|}\left[\tilde{e} - \frac{t}{4m^2}\tilde{h}\right] \mp \frac{m^2}{\xi|P_\perp|}\left[e - \frac{t}{4m^2}h\right],
\end{aligned}
\tag{34}
$$

where $\xi\equiv\xi_{\rm BMP}$ is defined in Eq. (6). Making use of these relations it is straightforward to obtain the expressions for the CFFs as linear combinations of the invariant functions $V_{0,1,2}^{(1,2,3)}$, $A_{0,1,2}^{(1,2,3)}$ from the previous section.

In the DVCS phenomenology a different decomposition of the Compton amplitude is traditionally used, being a certain generalization of the standard DIS reference frame where the initial photon and proton momenta form the longitudinal plane. Several conventions based on this identification exist and are in practice very similar to each other. The KM convention used by Kumericki and Müller in global DVCS leading-twist fits is one such example. Belitsky, Müller and Ji (BMJ) [37] used the KM decomposition to derive explicit expressions for key DVCS observables including subleading-power CFFs.

The main difference to BMP conventions is that KM (and BMJ) define helicity amplitudes in the target rest frame and to this end, introduce different sets of polarization vectors for the initial and final state photons. Also the definition of the skewness variable is different, $\xi_{\rm KM} = x_B/(2-x_B)$. The relation between the BMP and KM (BMJ) CFFs is just a Lorentz transformation and can easily be worked out, see [24]

$$
\begin{aligned}
\mathcal{F}^{\pm+}_{\rm KM} &= \mathcal{F}^{\pm+}_{\rm BMP} + \frac{\varkappa}{2}[\mathcal{F}^{++}_{\rm BMP} + \mathcal{F}^{-+}_{\rm BMP}] - \varkappa_0\mathcal{F}^{0+}_{\rm BMP},\\
\mathcal{F}^{0+}_{\rm KM} &= -(1+\varkappa)\mathcal{F}^{0+}_{\rm BMP} + \varkappa_0[\mathcal{F}^{++}_{\rm BMP} + \mathcal{F}^{-+}_{\rm BMP}],
\end{aligned}
\tag{35}
$$

etc. Here all entries $\mathcal{F}\in\{\mathcal{H},\mathcal{E},\tilde{\mathcal{H}},\tilde{\mathcal{E}}\}$ are functions of x_B, t, Q^2. Also

$$\varkappa_0 = \frac{\sqrt{2}Q\tilde{K}}{\sqrt{1+\gamma^2}(Q^2+t)} = \mathcal{O}(1/Q),$$
$$\varkappa = \frac{Q^2 - t + 2x_B t}{\sqrt{1+\gamma^2}(Q^2+t)} - 1 = \mathcal{O}(1/Q^2), \qquad (36)$$

where

$$\gamma = 2mx_B/Q, \qquad \tilde{K} = x_B(1+t/Q^2)|P_\perp|. \qquad (37)$$

These relations are exact, there is no approximation.

Note that the power counting $\mathcal{F}^{++} = \mathcal{O}(1/Q^0)$, $\mathcal{F}^{0+} = \mathcal{O}(1/Q)$, and $\mathcal{F}^{-+} = \mathcal{O}(1/Q^2)$, remains the same for both, BMP and BMJ, versions. In particular the difference between the leading, helicity conserving amplitudes, is a higher-twist effect. Numerically, however, the difference can be significant since the kinematic factors $\varkappa, \varkappa_0$ are rather large in the experimentally relevant kinematics, notwithstanding that they are formally power-suppressed. The numerical results presented below are obtained by using the set of BMP CFFs including kinematic power corrections to twist-six accuracy, Sec. II C, transforming them to the BMJ CFF basis (35), and calculating DVCS observables using the expressions provided in Ref. [37].

IV. DVCS OBSERVABLES

To evaluate observables, we need to express the electroproduction cross sections in terms of the BMP CFFs $\mathcal{F}_{\rm BMP}$. Instead of a direct calculation, we follow the procedure used in Ref. [24], transforming BMP CFFs to the KM (BMJ) basis, $\mathcal{F}_{\rm BMP} \to \mathcal{F}_{\rm KM}$, and making use of the results from Ref. [37]. This transformation is straightforward and can be thought of as, loosely speaking, a Lorentz transformation to a different reference frame.

The results of a numerical calculation presented below are obtained using the GPD model GK12 Goloskokov and Kroll [41]. It is based on the Radyushkin's double distribution ansatz [3] and also involves a certain model for an approximate Q^2 dependence. It is convenient for our purposes as all needed ξ derivatives can be evaluated analytically.

As an example, we consider the helicity-conserving CFF $\mathcal{H}^{++}(x_B, t, Q^2)$ which gives the dominant contribution to the DVCS cross section for the unpolarized target. The results for the absolute value and phase of $\mathcal{H}^{++}_{\rm BMP}(x_B, t, Q^2)$ and $\mathcal{H}^{++}_{\rm KM}(x_B, t, Q^2)$ are shown in Figs. 1 and 2, respectively. We choose $Q^2 = 3$ GeV^2 and present, in both cases, the results of the calculation with and without power corrections as functions of t for fixed value $x_B = 0.15$ (left panels), $x_B = 0.30$ (middle), and, alternatively, as functions of x_B for fixed $t = -0.75$ GeV^2 (right panels). As already mentioned, in this work we define the twist expansion as power counting in $(qq') = -1/2(Q^2+t)$ which implies that a part of the $1/Q^4$ corrections is included already in the twist-4 term. The remaining twist-6 contributions remain small up to $|t|/Q^2 \sim 1/4$ but increase rapidly for larger momentum transfers.

As another example, we consider the higher-twist helicity-flip CFF $\mathcal{H}^{0+}(x_B, t, Q^2)$ with a longitudinal virtual photon in the initial state. This CFF starts at twist-3 level, $\mathcal{H}^{0+} \sim 1/Q$. The corresponding (kinematic) contribution is traditionally referred to as the Wandzura-Wilczek (WW) approximation. The new contribution of this work is the calculation of the subleading power twist-5 correction $\sim 1/Q^3$. The results in the BMP reference frame are shown in Fig. 3. The twist-5 contributions are significant and become of the same order as the WW twist-3 term already at $|t|/Q^2 \sim 0.3$. The corresponding KM CFFs $\mathcal{H}^{0+}_{\rm KM}$

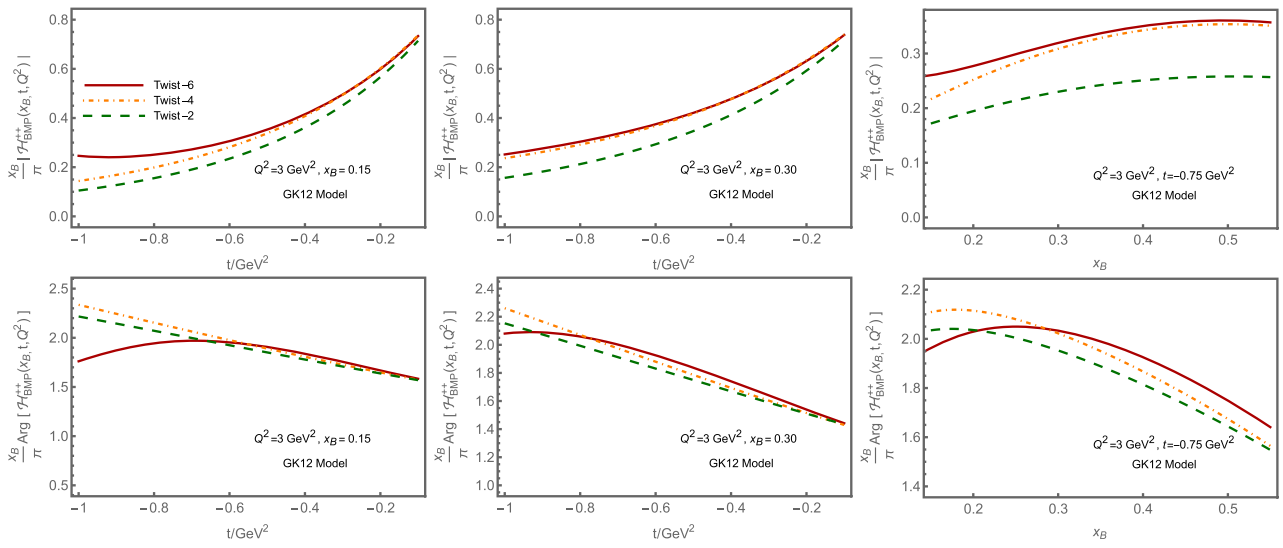

FIG. 1. Kinematic power corrections to the absolute value and phase of the BMP Compton form factor $\mathcal{H}^{++}_{\rm BMP}(x_B, t, Q^2)$.

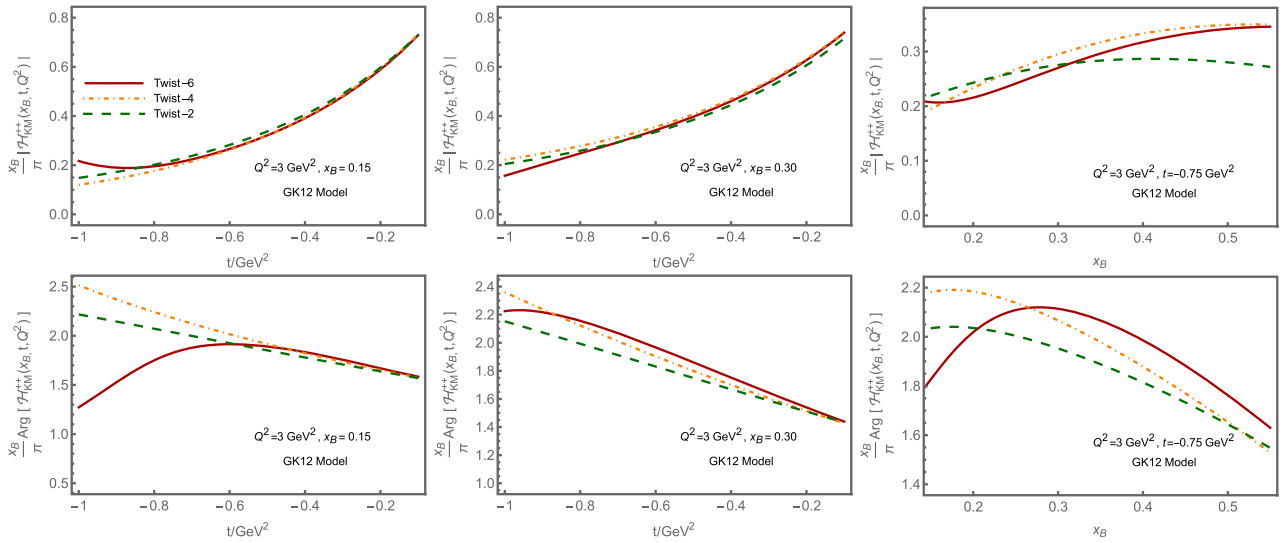

FIG. 2. Kinematic power corrections to the absolute value and phase of the KM Compton form factor $\mathcal{H}^{++}_{\rm KM}(x_B, t, Q^2)$.

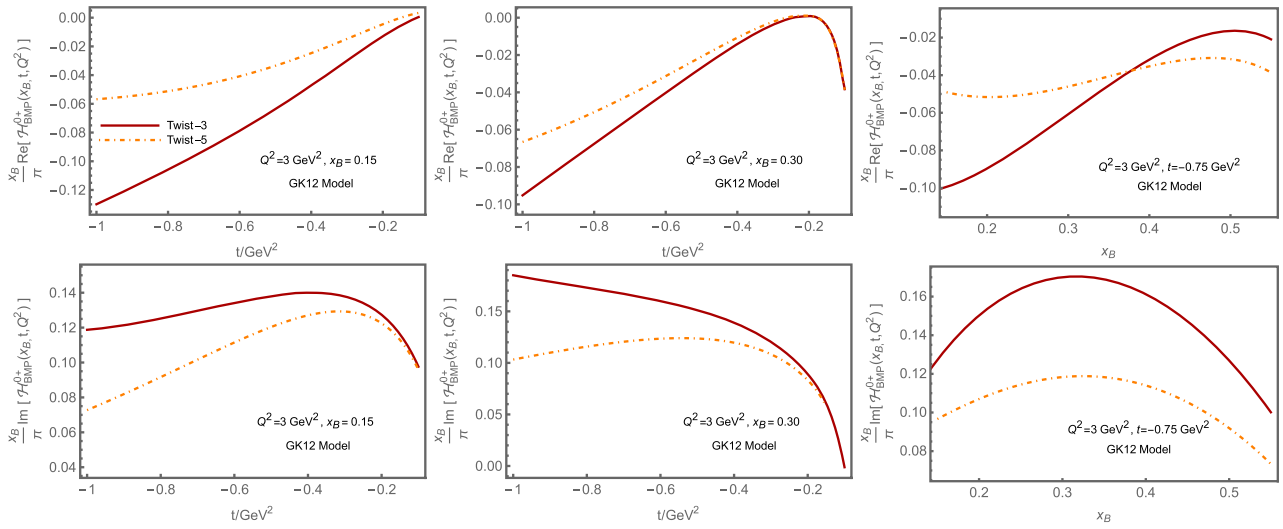

FIG. 3. Real (upper panels) and imaginary (lower panels) parts of the helicity-flip BMP Compton form factor $\mathcal{H}^{0+}_{\rm BMP}(x_B, t, Q^2)$.

obtained from $\mathcal{H}^{0+}_{\rm BMP}$ using the relation in Eq. (35) are shown in Fig. 4. By this transformation, contributions of different twists get mixed. For example, the WW twist-3 contribution in the KM frame is obtained as a sum of the twist-3 contribution in the BMP frame and the BMP twist-2 CFF decorated by a kinematic factor $\varkappa_0 \sim \sqrt{-t}/Q$, $\mathcal{H}^{0+}_{\rm KM} = -\mathcal{H}^{0+}_{\rm BMP} + \varkappa_0 \mathcal{H}^{++}_{\rm BMP} + \cdots$ where the ellipses stand for the terms $\sim 1/Q^3$ and higher powers. These two contributions tend to have an opposite sign so that a larger $\mathcal{H}^{0+}_{\rm BMP}$ generally leads to a smaller $\mathcal{H}^{0+}_{\rm KM}$, see Fig. 4. In these plots we do not perform a systematic power expansion, but show instead the results for $\mathcal{H}^{0+}_{\rm BMP}$ calculated using Eq. (35) literally, with a certain approximation for the BMP CFFs $\mathcal{H}^{++}_{\rm BMP}$, $\mathcal{H}^{0+}_{\rm BMP}$, $\mathcal{H}^{-+}_{\rm BMP}$ as inputs. The dashed curves are obtained by using the leading-twist approximation for $\mathcal{H}^{++}_{\rm BMP}$ and putting the other two BMP CFFs to zero; the dash-dotted curves are obtained using all three BMP CFFs to twist-4 accuracy, and the solid curves show the final results including the twist-5 and twist-6 terms. The higher-twist corrections are large in all cases and have a nontrivial pattern. However, the helicity flip CFF is small in comparison to the helicity-conserving one, cf. Fig. 2, so that the results for the cross sections and spin asymmetries are not affected strongly.

In the last years new experimental data on DVCS from Jefferson Lab have appeared, with extended Q^2 and x_B phase space reached including considerably smaller statistical uncertainty as compared to previous results. In Fig. 5 we compare our results on the kinematic power corrections to the spin-averaged DVCS cross section with the Hall A results [32]. As above, we use the GK12 GPD model as an

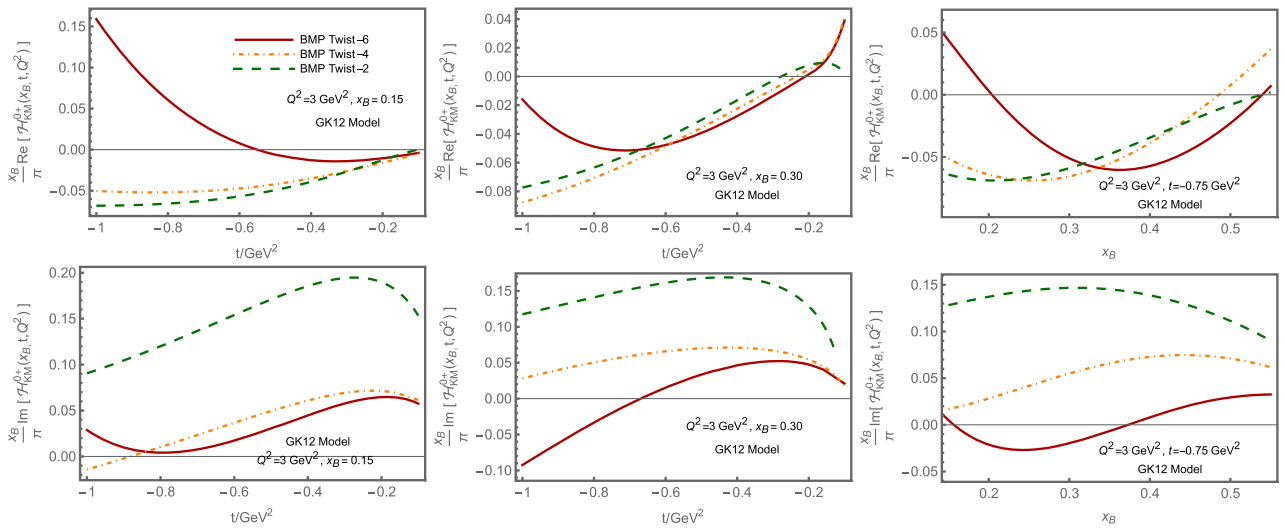

FIG. 4. Real (upper panels) and imaginary (lower panels) parts of the helicity-flip KM Compton form factor $\mathcal{H}^{0+}_{\mathrm{KM}}(x_B, t, Q^2)$.

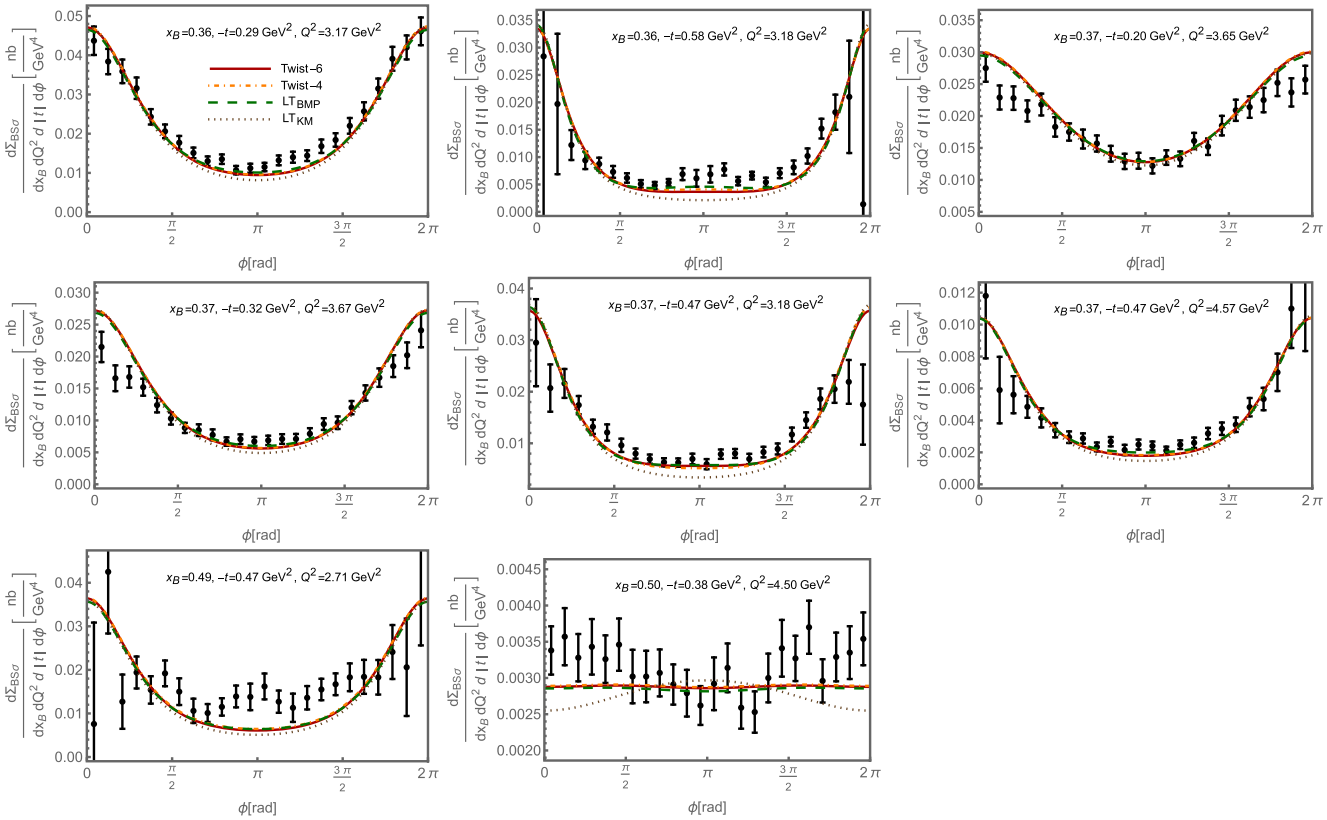

FIG. 5. Spin-averaged cross sections from Jefferson Lab HallA [32] (selected datasets).

example, and take into account Bethe-Heitler contributions as in Ref. [24]. The dotted and dashed curves are calculated in the leading-twist approximation defined in the KM and BMP reference frames, the dash-dotted curve shows the calculation with twist-4 corrections included, and the solid curve presents the full result to twist-6 accuracy. We have chosen for this figure the Hall A datasets with larger $|t|/Q^2$ values where the power corrections are more important, but avoid the ones with the largest x_B values as the GK12 model was not fitted to this range. The target mass corrections prove to be negligible for all considered cases.

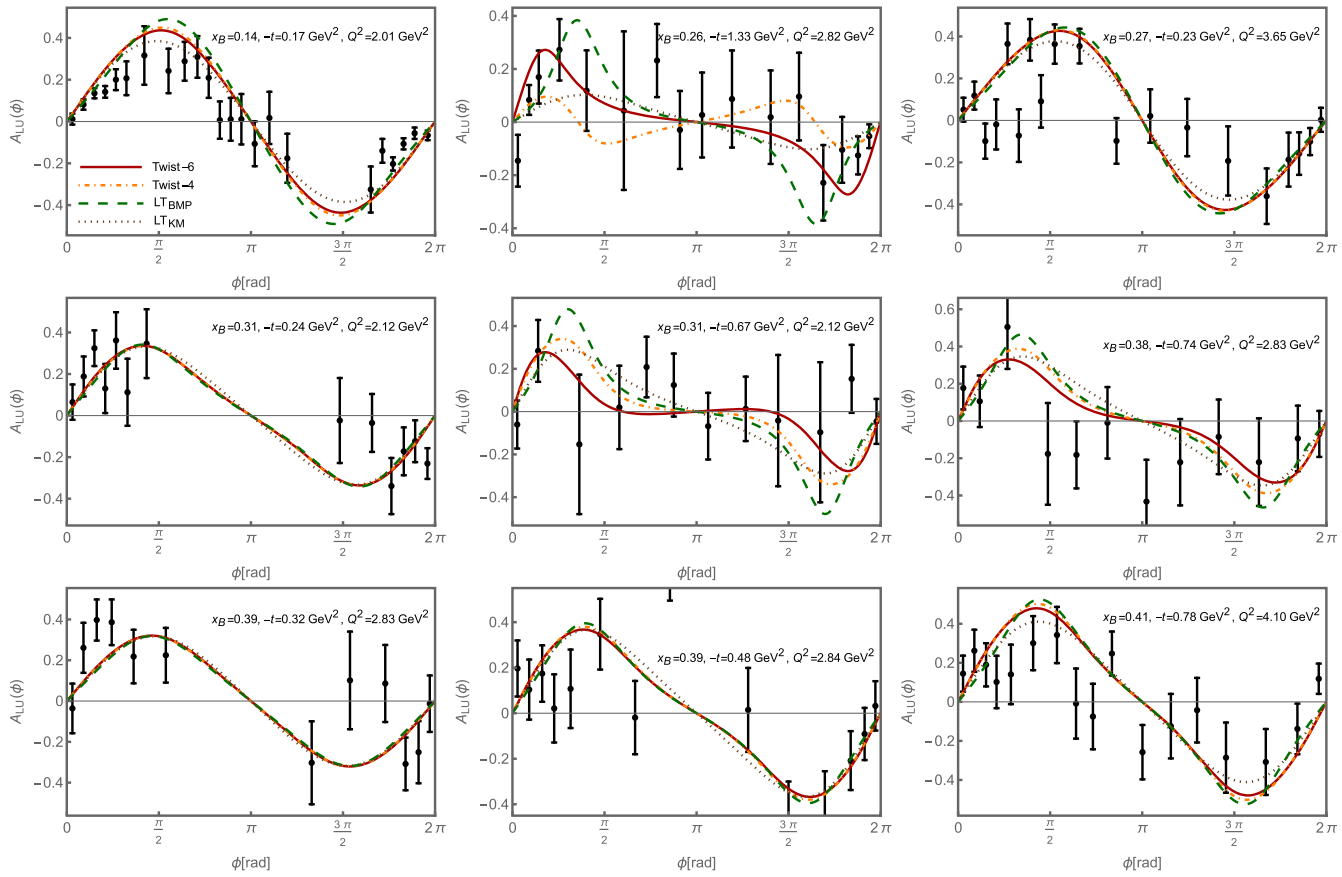

FIG. 6. Beam spin asymmetries from Jefferson Lab CLAS12 10.6 GeV dataset [42] (selected datasets).

In Ref. [42] the first measurement of the DVCS beam-spin asymmetry was reported using the CLAS12 spectrometer with a 10.2 and 10.6 GeV electron beam scattering off unpolarized protons. Our results in several different approximations are compared with their selected datasets in Fig. 6. Note that there are several datasets with large values of the momentum transfer $|t|/Q^2 \sim 0.5$ in which case the power corrections become very large, but, in general, their size is moderate and the overall agreement with the data appears to be quite satisfactory. In the future, it would be very interesting to see the spin-averaged cross section measurements from CLAS12 in a similar broad t-range.

V. CONCLUSIONS

We have studied kinematic power corrections to the DVCS observables including, for the first time, the contributions of twist-5 and twist-6 to the Compton form factors. The motivation for this work is provided by the three-dimensional "tomographic" imaging program of the proton and light nuclei, with the generalized parton distributions encoding the information on the transverse position of quarks and gluons in the proton in dependence on their longitudinal momentum. The resolving power on the transverse distance is directly limited by the range of the invariant moment transfer t which can be used in the analysis. Thus the theoretical control over power corrections $(\sqrt{-t}/Q)^k$ is crucial.

The main thrust of the present calculation has been to find out the range of momentum transfers for which the hierarchy of contributions with different power suppression holds, i.e., the twist-5,6 contributions are still smaller than twist-3,4 ones. Our results suggest that for $|t|/Q^2 \lesssim 1/4$ the twist expansion is converging for most observables, confirming the previous estimate from Ref. [23] that was based on the hierarchy of the leading twist-2 and twist-3,4 terms. However, $1/(qq') = 2/(Q^2+t)$ appears to be a better expansion parameter as compared to the nominal hard scale $1/Q^2$.

Apart from that, we present additional evidence that target mass corrections $\sim(m/Q)^k$ do not spoil QCD factorization for coherent DVCS on nuclei. The reason is that such contributions to Compton form factors always involve additional factors of the skewness parameter, so that the expansion goes in powers of $\xi^2 m^2/Q^2$ rather than m^2/Q^2. This feature was already observed in Ref. [23] to twist-4 accuracy, and is now confirmed up to twist-6. For nuclear targets, effectively, $m \to Am$ and $\xi \to \xi/A$, so that the target mass corrections remain essentially the same as for the nucleon and are small, apart from the large x_B region.

ACKNOWLEDGMENTS

We thank K. Kumericki for a discussion of the GPD models. This work was supported by the Research Unit FOR2926 funded by the Deutsche Forschungsgemeinschaft (DFG, German Research Foundation) under Grant No. 409651613. Y. J. acknowledges the support of the University Development Fund (UDF) of The Chinese University of Hong Kong, Shenzhen, under Grant No. UDF01003869, and the DFG through the Sino-German Collaborative Research Center TRR110 (DFG Project-ID 196253076, NSFC Grant No. 12070131001, —TRR 110).

DATA AVAILABILITY

No data were created or analyzed in this study.

APPENDIX: HELICITY AMPLITUDES IN THE DOUBLE DISTRIBUTION REPRESENTATION

At the intermediate stages of the calculation the following "double distribution" (DD) [3] parametrization of the nucleon matrix elements of light-ray vector- and axial-vector operators proves to be the most convenient

$$\begin{aligned}\mathcal{O}_V(z_1 n, z_2 n) &= \iint dydz e^{iyP_+ z_{12} + i\frac{1}{2}\Delta_+(z_1+z_2-z_{12}z)} \\ &\times \left\{ v_+ h_-(y,z,t) + \frac{i(vP)}{z_{12}m^2}\mathbf{\Phi}_+(y,z,t)\right\}, \\ \mathcal{O}_A(z_1 n, z_2 n) &= \iint dydz e^{iyP_+ z_{12} + i\frac{1}{2}\Delta_+(z_1+z_2-z_{12}z)} \\ &\times \left\{ a_+ \tilde{h}_+(y,z,t) + \frac{i(a\Delta)}{2z_{12}m^2}\tilde{\mathbf{\Phi}}_-(y,z,t)\right\}.\end{aligned} \tag{A1}$$

The variables x, y are related to the original Radyushkin's notation as $y \equiv \beta$ and $z \equiv \alpha$, and the integration goes over the region $|y| + |z| \le 1$. The subscripts $\pm$ of the DDs (boldface) indicate parity under the $(y,z) \mapsto (-y,-z)$ transformation, namely

$$\begin{aligned} h_-(y,z,t) &= -h_-(-y,-z,t), \\ \tilde{h}_+(y,z,t) &= \tilde{h}_+(-y,-z,t), \end{aligned} \tag{A2}$$

etc. The DD $\tilde{\mathbf{\Phi}}_-$ is an odd function of z whereas all other DDs are even functions of z. The DDs $\mathbf{\Phi}_+$ and $\tilde{\mathbf{\Phi}}_-$ can alternatively be written as [43]

$$\begin{aligned} \mathbf{\Phi}_+(y,z) &= \partial_y f(y,z) + \partial_z g(y,z), \\ \tilde{\mathbf{\Phi}}_-(y,z) &= \partial_y \tilde{f}(y,z) + \partial_z \tilde{g}(y,z). \end{aligned} \tag{A3}$$

The "standard" GPDs $H, E, \tilde{H}, \tilde{E}$ (12) can be expressed in terms of the DDs defined above as follows [23],

$$\begin{aligned}(H+E)(x,\xi,t) &= \iint dydz\delta(x-y-\xi z) h_-(y,z,t), \\ -E(x,\xi,t) &= \iint dydz\delta(x-y-\xi z) \\ &\times (f(y,z,t) + \xi g(y,z,t)), \\ \tilde{H}(x,\xi,t) &= \iint dydz\delta(x-y-\xi z)\tilde{h}_+(y,z,t), \\ -\tilde{E}(x,\xi,t) &= \frac{1}{\xi}\iint dydz\delta(x-y-\xi z) \\ &\times (\tilde{f}(y,z,t) + \xi\tilde{g}(y,z,t)).\end{aligned} \tag{A4}$$

The calculation follows the same routine as for a scalar target [34], but is more cumbersome due to a proliferation of Lorentz structures. In the expressions given below $h_- \equiv h_-(y,z)$, $\tilde{h}_+ \equiv \tilde{h}_+(y,z)$, etc. We use rescaled variables $\hat{t}$, $\hat{m}^2$, $|\hat{P}_\perp|^2$ defined in Eq. (21) and the notation

$$\mathcal{D}_w \equiv y\partial_w, \tag{A5}$$

where

$$\begin{aligned} w \equiv w(y,z) &= \frac{1}{2}\left(\frac{y}{\xi} + z + 1\right), \\ w(-y,-z) &= 1 - w(y,z). \end{aligned} \tag{A6}$$

The coefficient functions are defined in Eq. (25).

We write the result for the helicity-conserving amplitude $\mathcal{A}^{\pm\pm}_{A,V}$ as a sum of four terms following the notation in Eq. (26). We obtain

$$\begin{aligned} V_0^{(1)} = \iint dydz h_- \Bigg\{ &-\left(1+\frac{\hat{t}}{4}\right)T_0(w) - \frac{\hat{t}}{2}T_{10}(w) + \left[\hat{t}\left(1+\frac{1}{\xi}\mathcal{D}_w\right) - \frac{1}{2}|\hat{P}_\perp|^2\mathcal{D}_w{}^2\right][T_2(w) + 2\hat{t}T_V(w)] \\ &+ \frac{\hat{t}^2}{4}T_{11}(w) + \left[\frac{3}{2}\hat{t}\left(1+\frac{1}{2\xi}\mathcal{D}_w\right)\left(\frac{\hat{t}}{\xi} - |\hat{P}_\perp|^2\mathcal{D}_w\right)\mathcal{D}_w + \frac{1}{8}|\hat{P}_\perp|^4\mathcal{D}_w{}^4\right]T_3(w)\Bigg\}, \end{aligned} \tag{A7a}$$

$$V_0^{(2)} = \iint dydz\mathbf{\Phi}_+\Big\{\Big(1+\frac{\hat{t}}{4}\Big)T_1(w)+\frac{\hat{t}}{2}\mathrm{Li}_2(w)+\frac{1}{2}y\Big(\frac{\hat{t}}{\xi}-|\hat{P}_\perp|^2\mathcal{D}_w\Big)T_2(w)+\frac{\hat{t}^2}{4}(\mathrm{Li}_2(w)-2\bar{w}\ln\bar{w})$$
$$+y\hat{t}\Big(\frac{\hat{t}}{\xi}-|\hat{P}_\perp|^2\mathcal{D}_w\Big)T_V(w)-\frac{1}{2}y\Big[-\frac{\hat{t}^2}{2\xi^2}+\hat{t}|\hat{P}_\perp|^2\Big(1+\frac{1}{\xi}\mathcal{D}_w\Big)-\frac{1}{4}|\hat{P}_\perp|^4{\mathcal{D}_w}^2\Big]\mathcal{D}_wT_3(w)\Big\}$$
$$-\hat{m}^2\iint dydzh_-\Big\{\mathcal{D}_w(T_2(w)+2\hat{t}\mathrm{T}_V(w))-\Big[\hat{t}\Big(1+\frac{1}{\xi}\mathcal{D}_w\Big)-\frac{1}{2}|\hat{P}_\perp|^2{\mathcal{D}_w}^2\Big]T_3(w)\Big\} \tag{A7b}$$

$$A_0^{(1)} = \iint dydz\tilde{h}_+\Big\{\Big(1+\frac{\hat{t}}{4}\Big)T_0(w)+\frac{\hat{t}}{2}T_{10}(w)-\Big[\hat{t}\Big(1+\frac{1}{\xi}\mathcal{D}_w\Big)-\frac{1}{2}|\hat{P}_\perp|^2{\mathcal{D}_w}^2\Big][T_2(w)-2\hat{t}T_A(w)]$$
$$+\frac{\hat{t}^2}{4}T_{10}(w)+\frac{9}{2}\Big[\hat{t}\Big(1+\frac{1}{2\xi}\mathcal{D}_w\Big)\Big(\frac{\hat{t}}{\xi}-|\hat{P}_\perp|^2\mathcal{D}_w\Big)+\frac{1}{12}|\hat{P}_\perp|^4{\mathcal{D}_w}^3\Big]\mathcal{D}_w\Big[T_A(w)-\frac{1}{2}T_{00}(w)\Big]\Big\}, \tag{A8a}$$

$$A_0^{(2)} = \iint dydz\tilde{\mathbf{\Phi}}_-\Big\{-\Big(1+\frac{\hat{t}}{4}\Big)T_1(w)-\frac{\hat{t}}{2}\mathrm{Li}_2(w)-\frac{1}{2}y\Big(\frac{\hat{t}}{\xi}-|\hat{P}_\perp|^2\mathcal{D}_w\Big)[T_2(w)-2\hat{t}T_A(w)]$$
$$-\frac{\hat{t}^2}{4}\Big(\mathrm{Li}_2(w)-\frac{3}{2}w\Big)+\frac{3}{4}y\Big[\frac{\hat{t}^2}{\xi^2}-2\hat{t}|\hat{P}_\perp|^2\Big(1+\frac{1}{\xi}\mathcal{D}_w\Big)+\frac{1}{2}|\hat{P}_\perp|^4{\mathcal{D}_w}^2\Big]\mathcal{D}_w\Big[T_A(w)-\frac{1}{2}T_{00}(w)\Big]\Big\}$$
$$+2\hat{m}^2\iint dydz\tilde{h}_+\Big\{\Big(1+\frac{1}{2\xi}\mathcal{D}_w\Big)[T_2(w)-2\hat{t}T_A(w)]$$
$$-\frac{3}{2}\Big[\frac{\hat{t}}{\xi}+\frac{|\hat{P}_\perp|^2}{2\xi}{\mathcal{D}_w}^2+2\Big(\frac{\hat{t}}{\xi}-|\hat{P}_\perp|^2\mathcal{D}_w\Big)\Big(1+\frac{1}{2\xi}\mathcal{D}_w\Big)\Big]\mathcal{D}_w\Big[T_A(w)-\frac{1}{2}T_{00}(w)\Big]\Big\}. \tag{A8b}$$

Helicity-flip amplitudes $\mathcal{A}_{A,V}^{0\pm}$ can be written as sum of six invariant functions defined in Eq. (28)

$$V_1^{(1)} = \iint dydzh_-\Big\{-T_{10}(w)+\frac{\hat{t}}{2}T_{11}(w)+\Big[\hat{t}\Big(1+\frac{1}{\xi}\mathcal{D}_w\Big)-\frac{1}{2}|\hat{P}_\perp|^2{\mathcal{D}_w}^2\Big]T_V(w)\Big\}, \tag{A9a}$$

$$V_1^{(2)} = \iint dydzh_-\Big\{\mathcal{D}_wT_{10}(w)-\frac{\hat{t}}{2}\mathcal{D}_wT_{11}(w)-3\Big[\hat{t}\Big(1+\frac{1}{2\xi}\mathcal{D}_w\Big)-\frac{1}{6}|\hat{P}_\perp|^2{\mathcal{D}_w}^2\Big]\mathcal{D}_wT_V(w)\Big\}, \tag{A9b}$$

$$V_1^{(3)} = \iint dydzy\mathbf{\Phi}_+\Big\{T_{10}(w)-\frac{\hat{t}}{2}T_{11}(w)-\Big[\hat{t}\Big(1+\frac{1}{\xi}\mathcal{D}_w\Big)-\frac{1}{2}|\hat{P}_\perp|^2{\mathcal{D}_w}^2\Big]T_V(w)\Big\}+\hat{m}^2\iint dydzh_-{\mathcal{D}_w}^2T_V(w), \tag{A9c}$$

$$A_1^{(1)} = \iint dydz\tilde{h}_+\Big\{\Big(1+\frac{\hat{t}}{2}\Big)T_{10}(w)+\Big[\hat{t}\Big(1+\frac{1}{\xi}\mathcal{D}_w\Big)-\frac{1}{2}|\hat{P}_\perp|^2{\mathcal{D}_w}^2\Big]T_A(w)\Big\}, \tag{A10a}$$

$$A_1^{(2)} = \iint dydz\tilde{h}_+\Big\{-\Big(1+\frac{\hat{t}}{2}\Big)\mathcal{D}_wT_{10}(w)-3\Big[\hat{t}\Big(1+\frac{1}{2\xi}\mathcal{D}_w\Big)-\frac{1}{6}|\hat{P}_\perp|^2{\mathcal{D}_w}^2\Big]\mathcal{D}_wT_A(w)\Big\}, \tag{A10b}$$

$$A_1^{(3)} = \iint dydzy\tilde{\mathbf{\Phi}}_-\Big\{-\Big(1+\frac{\hat{t}}{2}\Big)T_{10}(w)-\Big[\hat{t}\Big(1+\frac{1}{\xi}\mathcal{D}_w\Big)-\frac{1}{2}|\hat{P}_\perp|^2{\mathcal{D}_w}^2\Big]T_A(w)\Big\}$$
$$+4\hat{m}^2\iint dydz\tilde{h}_+\Big(1+\frac{1}{4\xi}\mathcal{D}_w\Big)\mathcal{D}_wT_A(w). \tag{A10c}$$

Finally, the amplitudes $\mathcal{A}_{A,V}^{\mp\pm}$ with helicity flip by two units, can be written as a sum of 6 terms as in Eq. (30). We get

$$V_2^{(1)} = \iint dydzh_-\Big\{2\Big(1+\frac{\hat{t}}{4}\Big)\mathcal{D}_wT_{11}(w)+3\Big[\hat{t}\Big(1+\frac{1}{2\xi}\mathcal{D}_w\Big)-\frac{1}{6}|\hat{P}_\perp|^2{\mathcal{D}_w}^2\Big]\mathcal{D}_wT_V(w)\Big\}, \tag{A11a}$$

$$V_2^{(2)} = |\hat{P}_\perp|^2\iint dydzh_-\Big\{-\frac{1}{2}\Big(1+\frac{\hat{t}}{4}\Big){\mathcal{D}_w}^2T_{11}(w)-\frac{3}{2}\Big[\hat{t}\Big(1+\frac{1}{3\xi}\mathcal{D}_w\Big)-\frac{1}{12}|\hat{P}_\perp|^2{\mathcal{D}_w}^2\Big]{\mathcal{D}_w}^2T_V(w)\Big\}, \tag{A11b}$$

$$V_2^{(3)} = |\hat{P}_\perp|^2 \iint dydzy\Phi_+ \left\{ -\frac{1}{2}\left(1+\frac{\hat{t}}{4}\right)\mathcal{D}_w T_{11}(w) - \frac{3}{4}\left[\hat{t}\left(1+\frac{1}{2\xi}\mathcal{D}_w\right) - \frac{1}{6}|\hat{P}_\perp|^2 \mathcal{D}_w{}^2\right]\mathcal{D}_w T_V(w)\right\}$$
$$+ \frac{1}{4}|\hat{P}_\perp|^2 \hat{m}^2 \iint dydzh_- \mathcal{D}_w{}^3 T_V(w), \tag{A11c}$$

$$A_2^{(1)} = \iint dydz\tilde{h}_+ \left\{ 2\left(1+\frac{\hat{t}}{4}\right)\mathcal{D}_w T_{10}(w) + 3\left[\hat{t}\left(1+\frac{1}{2\xi}\mathcal{D}_w\right) - \frac{1}{6}|\hat{P}_\perp|^2 \mathcal{D}_w{}^2\right]\mathcal{D}_w T_A(w)\right\}, \tag{A12a}$$

$$A_2^{(2)} = |\hat{P}_\perp|^2 \iint dydz\tilde{h}_+ \left\{ -\frac{1}{2}\left(1+\frac{\hat{t}}{4}\right)\mathcal{D}_w{}^2 T_{10}(w) - \frac{3}{2}\left[\hat{t}\left(1+\frac{1}{3\xi}\mathcal{D}_w\right) - \frac{1}{12}|\hat{P}_\perp|^2 \mathcal{D}_w{}^2\right]\mathcal{D}_w{}^2 T_A(w)\right\}, \tag{A12b}$$

$$A_2^{(3)} = |\hat{P}_\perp|^2 \iint dydzy\tilde{\mathbf{\Phi}}_- \left\{ -\frac{1}{2}\left(1+\frac{\hat{t}}{4}\right)\mathcal{D}_w T_{10}(w) - \frac{3}{4}\left[\hat{t}\left(1+\frac{1}{2\xi}\mathcal{D}_w\right) - \frac{1}{6}|\hat{P}_\perp|^2 \mathcal{D}_w{}^2\right]\mathcal{D}_w T_A(w)\right\}$$
$$+ \frac{3}{2}|\hat{P}_\perp|^2 \hat{m}^2 \iint dydz\tilde{h}_+ \left(1+\frac{1}{6\xi}\mathcal{D}_w\right)\mathcal{D}_w{}^2 T_A(w). \tag{A12c}$$

Starting from these expressions, it is straightforward to rewrite the results in terms of GPDs using the following identities:

$$\iint dydz\mathbf{\Phi}_+(y,z)Y(w) = \frac{1}{2\xi}\int dxY'\left(\frac{x+\xi}{2\xi}\right)E(x,\xi,t),$$
$$\iint dydz\tilde{\mathbf{\Phi}}_-(y,z)Y(w) = \frac{1}{2}\int dxY'\left(\frac{x+\xi}{2\xi}\right)\tilde{E}(x,\xi,t),$$
$$\iint dydzy\mathbf{\Phi}_+(y,z)\mathcal{D}_w{}^k Y(w) = (-2\xi^2\partial_\xi)^{k+1}\frac{1}{2\xi}\int dxY\left(\frac{x+\xi}{2\xi}\right)E(x,\xi,t),$$
$$\iint dydzy\tilde{\mathbf{\Phi}}_-(y,z)\mathcal{D}_w{}^k Y(w) = (-2\xi^2\partial_\xi)^{k+1}\frac{1}{2}\int dxY\left(\frac{x+\xi}{2\xi}\right)\tilde{E}(x,\xi,t),$$
$$\iint dydzh_-(y,z)\mathcal{D}_w{}^k Y(w) = (-2\xi^2\partial_\xi)^k \int dxY\left(\frac{x+\xi}{2\xi}\right)(H(x,\xi,t)+E(x,\xi,t)),$$
$$\iint dydz\tilde{\mathbf{h}}_+(y,z)\mathcal{D}_w{}^k Y(w) = (-2\xi^2\partial_\xi)^k \int dxY\left(\frac{x+\xi}{2\xi}\right)\tilde{H}(x,\xi,t), \tag{A13}$$

where $Y(w)$ is an arbitrary function. The final results in the GPD representation are given in Sec. II C.

[1] D. Müller, D. Robaschik, B. Geyer, F. M. Dittes, and J. Hořejši, Wave functions, evolution equations and evolution kernels from light ray operators of QCD, Fortschr. Phys. **42**, 101 (1994).

[2] X.-D. Ji, Deeply virtual Compton scattering, Phys. Rev. D **55**, 7114 (1997).

[3] A. V. Radyushkin, Nonforward parton distributions, Phys. Rev. D **56**, 5524 (1997).

[4] R. Abdul Khalek *et al.*, Science requirements and detector concepts for the electron-ion collider: EIC Yellow Report, Nucl. Phys. **A1026**, 122447 (2022).

[5] R. Abdul Khalek *et al.*, Snowmass 2021 White Paper: Electron Ion Collider for High Energy Physics, in 2022 Snowmass Summer Study (2022), arXiv: 2203.13199.

[6] X.-D. Ji and J. Osborne, One loop corrections and all order factorization in deeply virtual Compton scattering, Phys. Rev. D **58**, 094018 (1998).

[7] A. V. Belitsky, A. Freund, and D. Müller, Evolution kernels of skewed parton distributions: Method and two loop results, Nucl. Phys. **B574**, 347 (2000).

[8] A. V. Belitsky and D. Müller, Broken conformal invariance and spectrum of anomalous dimensions in QCD, Nucl. Phys. **B537**, 397 (1999).

[9] J. D. Noritzsch, Heavy quarks in deeply virtual Compton scattering, Phys. Rev. D **69**, 094016 (2004).

[10] K. Kumericki, D. Müller, K. Passek-Kumericki, and A. Schäfer, Deeply virtual Compton scattering beyond next-to-leading order: The flavor singlet case, Phys. Lett. B **648**, 186 (2007).

[11] K. Kumericki, D. Müller, and K. Passek-Kumericki, Towards a fitting procedure for deeply virtual Compton scattering at next-to-leading order and beyond, Nucl. Phys. **B794**, 244 (2008).
[12] V. M. Braun, A. N. Manashov, S. Moch, and M. Strohmaier, Three-loop evolution equation for flavor-nonsinglet operators in off-forward kinematics, J. High Energy Phys. 06 (2017) 037.
[13] V. M. Braun, A. N. Manashov, S. Moch, and J. Schoenleber, Two-loop coefficient function for DVCS: Vector contributions, J. High Energy Phys. 09 (2020) 117; J. High Energy Phys.02 (2022) 115(E).
[14] V. M. Braun, A. N. Manashov, S. Moch, and J. Schoenleber, Axial-vector contributions in two-photon reactions: Pion transition form factor and deeply-virtual Compton scattering at NNLO in QCD, Phys. Rev. D **104**, 094007 (2021).
[15] J. Gao, T. Huber, Y. Ji, and Y.-M. Wang, Next-to-next-to-leading-order QCD prediction for the photon-pion form factor, Phys. Rev. Lett. **128**, 062003 (2022).
[16] V. M. Braun, K. G. Chetyrkin, and A. N. Manashov, NNLO anomalous dimension matrix for twist-two flavor-singlet operators, Phys. Lett. B **834**, 137409 (2022).
[17] V. M. Braun, Y. Ji, and J. Schoenleber, Deeply virtual Compton scattering at next-to-next-to-leading order, Phys. Rev. Lett. **129**, 172001 (2022).
[18] Y. Ji, A. Manashov, and S.-O. Moch, Evolution kernels of twist-two operators, Phys. Rev. D **108**, 054009 (2023).
[19] Y. Ji and J. Schoenleber, Two-loop coefficient functions in deeply virtual Compton scattering: Flavor-singlet axial-vector and transversity case, J. High Energy Phys. 01 (2024) 053.
[20] J. Schoenleber, Resummation of threshold logarithms in deeply-virtual Compton scattering, J. High Energy Phys. 02 (2023) 207.
[21] M. Hattawy *et al.* (CLAS Collaboration), First exclusive measurement of deeply virtual Compton scattering off ^{4}He: Toward the 3D tomography of nuclei, Phys. Rev. Lett. **119**, 202004 (2017).
[22] R. Dupré *et al.* (CLAS), Measurement of deeply virtual Compton scattering off ^{4}He with the CEBAF large acceptance spectrometer at Jefferson Lab, Phys. Rev. C **104**, 025203 (2021).
[23] V. M. Braun, A. N. Manashov, D. Müller, and B. Pirnay, Resolving kinematic ambiguities in QCD predictions for Deeply Virtual Compton Scattering, Proc. Sci., DIS2014 (**2014**) 225 [arXiv:1407.0815].
[24] V. M. Braun, A. N. Manashov, D. Müller, and B. M. Pirnay, Deeply virtual Compton scattering to the twist-four accuracy: Impact of finite-t and target mass corrections, Phys. Rev. D **89**, 074022 (2014).
[25] Y. Guo, X. Ji, and K. Shiells, Higher-order kinematical effects in deeply virtual Compton scattering, J. High Energy Phys. 12 (2021) 103.
[26] V. Braun and A. Manashov, Kinematic power corrections in off-forward hard reactions, Phys. Rev. Lett. **107**, 202001 (2011).
[27] V. Braun and A. Manashov, Operator product expansion in QCD in off-forward kinematics: Separation of kinematic and dynamical contributions, J. High Energy Phys. 01 (2012) 085.
[28] V. Braun, A. Manashov, and B. Pirnay, Finite-t and target mass corrections to DVCS on a scalar target, Phys. Rev. D **86**, 014003 (2012).
[29] V. Braun, A. Manashov, and B. Pirnay, Finite-t and target mass corrections to deeply virtual Compton scattering, Phys. Rev. Lett. **109**, 242001 (2012).
[30] M. Defurne *et al.* (Jefferson Lab Hall A Collaboration), E00-110 experiment at Jefferson Lab Hall A: Deeply virtual Compton scattering off the proton at 6 GeV, Phys. Rev. C **92**, 055202 (2015).
[31] M. Defurne *et al.*, A glimpse of gluons through deeply virtual Compton scattering on the proton, Nat. Commun. **8**, 1408 (2017).
[32] F. Georges *et al.* (Jefferson Lab Hall A Collaboration), Deeply virtual Compton scattering cross section at high Bjorken xB, Phys. Rev. Lett. **128**, 252002 (2022).
[33] V. M. Braun, Y. Ji, and A. N. Manashov, Two-photon processes in conformal QCD: Resummation of the descendants of leading-twist operators, J. High Energy Phys. 03 (2021) 051.
[34] V. M. Braun, Y. Ji, and A. N. Manashov, Next-to-leading-power kinematic corrections to DVCS: A scalar target, J. High Energy Phys. 01 (2023) 078.
[35] M. Diehl, Generalized parton distributions, Phys. Rep. **388**, 41 (2003).
[36] I. I. Balitsky and V. M. Braun, Evolution equations for QCD string operators, Nucl. Phys. **B311**, 541 (1989).
[37] A. V. Belitsky, D. Müller, and Y. Ji, Compton scattering: From deeply virtual to quasi-real, Nucl. Phys. **B878**, 214 (2014).
[38] I. I. Balitsky and V. M. Braun, The nonlocal operator expansion for inclusive particle production in e+ e- annihilation, Nucl. Phys. **B361**, 93 (1991).
[39] In Ref. [29] there is a sign error in the in-line equation after Eq. (7), it is corrected in [24] [Eq. (A11)].
[40] A. V. Belitsky, D. Mueller, and A. Kirchner, Theory of deeply virtual Compton scattering on the nucleon, Nucl. Phys. **B629**, 323 (2002).
[41] P. Kroll, H. Moutarde, and F. Sabatie, From hard exclusive meson electroproduction to deeply virtual Compton scattering, Eur. Phys. J. C **73**, 2278 (2013).
[42] G. Christiaens *et al.* (CLAS Collabroation), First CLAS12 measurement of deeply virtual Compton scattering beam-spin asymmetries in the extended valence region, Phys. Rev. Lett. **130**, 211902 (2023).
[43] O. V. Teryaev, Crossing and radon tomography for generalized parton distributions, Phys. Lett. B **510**, 125 (2001).